NIH Public Access
Author Manuscript

Frequency Dependence of Kidney Injury Induced by Contrast-Aided Diagnostic Ultrasound in Rats

Douglas L. Miller[1], **Chunyan Dou**[1], and **Roger C. Wiggins**[2]

[1]*Department of Radiology, University of Michigan, Ann Arbor MI 48109*

[2]*Department of Internal Medicine (Nephrology), University of Michigan, Ann Arbor MI 48109*

Abstract

This study was performed to examine the frequency dependence of glomerular capillary hemorrhage (GCH) induced by contrast aided diagnostic ultrasound in rats. Diagnostic ultrasound (DUS) scanners were utilized for exposure at 3.2, 5.0 and 7.4 MHz, and previously published data at 1.5 and 2.5 MHz also was included. A laboratory exposure system was used to simulate DUS exposure at 1.0, 1.5, 2.25, 3.5, 5.0 and 7.5 MHz with higher peak rarefactional pressure amplitudes (PRPAs) than were available from our DUS systems. The right kidneys of rats mounted in a water bath were exposed to intermittent image pulse sequences at 1 s intervals during infusion of diluted ultrasound contrast agent. The percentage of GCH was zero for low PRPAs, and then rapidly increased with increasing PRPAs above an apparent threshold, p_t. The values of p_t were approximately proportional to the ultrasound frequency, f, such that p_t/f was approximately 0.5 MPa/MHz for DUS and 0.6 MPa/MHz for laboratory-system exposures. The increasing thresholds with increasing frequency limited the GCH effect for contrast aided DUS, and no GCH was seen for DUS at 5.0 or 7.4 MHz for the highest available PRPAs.

Keywords

ultrasound contrast agent; diagnostic ultrasound adverse effects; acoustic cavitation; renal injury; mechanical index

Introduction and Literature

Ultrasound contrast agents (UCAs), which are suspensions of gas bodies (stabilized microbubbles), have been developed to enhance conventional ultrasound imaging in patients with sub-optimal examination results. Several extensive reviews describe UCA developments and applications (Averkiou, et al. 2003; Raisinghani et al. 2004; Blomley et al. 2007). Albunex® was the first transpulmonary UCA approved in the USA in 1994, and Levovist® was introduced in Europe in 1996 (Albrecht et al. 2004). Newer commercial UCAs are now in clinical usage; for example, Definity® (perflutren lipid microsphere injectable suspension, Brystol-Myers Squibb Medical Imaging, N. Billerica MA USA) approved in the USA in 2001 contains up to $1.2 \cdot 10^{10}$ microbubbles/ml of 1.1–3.3 µm diameter. The UCA are injected agents

Corresponding Author: Douglas Miller, RM 3315 Kresge III, University of Michigan Medical Center, 200 Zina Pitcher Place, Ann Arbor, MI 48109-0553, Telephone:(734) 647-3344, FAX: (734) 764-8541, Email: douglm@umich.edu.

and they have been evaluated primarily as drugs by the US Food and Drug Administration (USFDA), with restrictions to specific medical conditions. This separated approval process for the diagnostic ultrasound (DUS) imaging machines (e. g. using the 510(k) exemption in the USA) and the UCA (using pharmaceutical evaluation) leaves a fundamental problem concerning the interaction of imaging ultrasound exposure with a gas body. UCAs and special ultrasound imaging modes to utilize them present a challenge to safety assurance for diagnostic ultrasound (DUS) for two reasons. First, UCAs were developed, for the most part, after the landmark 1992 Output Display Standard (ODS) and the US Food and Drug Administration 510(k) guidelines for diagnostic ultrasound (DUS) imaging (AIUM/NEMA, 1992; FDA, 1997). Second, ultrasound actively interacts with the injected drugs, by activating the gas bodies and creating a novel cavitational device for diagnosis (or therapy). This problem apparently has impeded the UCA approval process and has lead to frustration within the diagnostic ultrasound community in the USA, which has solicited the USFDA for expedited approval of new UCAs and UCA applications (Greenbaum et al. 2007).

Prior to the development of UCAs, cavitation biology research could not be pursued *in vivo* for DUS-relevant conditions, because there appeared to be few, if any, suitable cavitation nuclei in living mammals. Theoretical analysis indicated that inertial cavitation thresholds for optimal nucleation were dependent on the ultrasonic frequency (Apfel and Holland, 1991). This theoretical result was used in creating the Mechanical Index (MI) exposure parameter for regulatory purposes in the ODS. The MI includes a dependence on frequency, f, as well as on the peak rarefactional pressure amplitude (PRPA), p_r, of imaging pulses and provides an estimate of the value of $p_r/f^{1/2}$ within the scanned tissue. The guideline upper limit was set at MI=1.9 for the 510(k) process (FDA, 1997), in accordance with legal requirements enacted in 1976. However, no thorough experimental database existed when the MI was developed, which could be used to confirm its utility for anticipating the occurrence or magnitude of cavitational bioeffects induced in mammals by DUS with UCA.

The invention of gas body UCAs qualitatively changed this situation, because UCA gas bodies can serve as virtually optimal cavitation nuclei. Physical nucleation of cavitation activity by UCAs has been shown *in vitro* (Miller and Thomas, 1995) and *in vivo* (Porter et al. 2001). New cavitation bioeffects data has gradually accumulated for conditions relevant to DUS with UCA, and has been the subject of several recent authoritative reviews (NCRP, 2002; Dalecki, 2007; Miller et al. in press). The *in situ* peak rarefactional pressure amplitude (PRPA) is the primary exposure parameter for cavitation. Estimating the equivalent MI is also important for relating bioeffects research to clinical DUS exposure, because this PRPA-related exposure parameter is displayed on most modern ultrasound scanners. Microscale bioeffects of cavitation activity in contrast DUS have been observed primarily for intermittent imaging, for which the gas bodies are destroyed and then allowed to re-fill the tissue before the next contrast-destructive image. These bioeffects include capillary leakage for moderate PRPAs, with capillary rupture and injury of adjacent parenchymal cells at higher PRPAs. At a given frequency, the microscale bioeffects also have been reported to depend on the agent, gas body dose, dose infusion rate, ultrasonic pulse duration, pulse repetition period, scan rate, intermittent interval, tissue perfusion, and other patient-related factors.

However, the available data on the frequency dependence of relevant bioeffects remains quite limited. *In vitro* studies with laboratory exposure systems indicate that cavitation thresholds are low relative to DUS upper limits and that thresholds for cellular bioeffects with UCAs increase with ultrasonic frequency more rapidly than $f^{1/2}$ (Miller et al, 1997; Dalecki et al. 1997; Miller and Dou, 2004a,b). These insights are important but cannot be related directly to *in vivo* DUS conditions with circulating contrast agent. Most *in vivo* studies of potential bioeffects of contrast ultrasound have employed diagnostic ultrasound scanners as the exposure source (Miller et al. in press), but only a few of these have provided information on the

frequency dependence of bioeffects. The induction of glomerular capillary hemorrhage (GCH) by diagnostic ultrasound exposure with Optison™ (or experimental agents designated MP-1950 and MP-2211) in the circulation was investigated by Wibble et al. (2002) using DUS imaging of rat kidneys at 1.8, 4.0 or 6 MHz. Capillary hemorrhage was scored by surface markings, and increased with increasing MI above apparent thresholds of about 0.6 and 1.0 (midway between the lowest exposure with the effect and the next lower level) at 1.8 and 4.0 MHz. The bioeffect was not produced at 6 MHz for the highest available exposure. There was some uncertainty in the actual *in situ* exposure in this study, because the probe was in contact with the rats (i. e., with the kidney center only about 1 cm away). In independent research, the GCH bioeffect was confirmed using Definity® with a 1.5 MHz probe scanning rats mounted in a water bath (to assure placement of the kidney at the focal maximum of the field) and the threshold was comparable at MI=0.6 (Miller et al. 2007a). In another study using a different DUS machine operating at 2.5 MHz, the apparent threshold for GCH was found to be MI=0.95 using similar *in vivo* conditions (Miller et al. 2007b). These studies of GCH induced by contrast DUS have indicated increasing thresholds for increasing ultrasound frequency, but only over a narrow range permitted by DUS machines, which complicates the accurate determination of the frequency dependence of cavitational bioeffects in DUS.

Laboratory exposure systems can expand parameter ranges beyond those available on clinical DUS systems. However, the confident extrapolation of results to the clinical problem requires the simulation of DUS exposure, which can be problematical with simple unscanned laboratory systems. For example, a laboratory exposure system was used to study induction of petechial hemorrhage in mouse intestine with UCA at different frequencies (Miller and Gies, 2000). However, unfocused fixed beams were energized with a simple pulse train, without allowing for intermittent refill of the tissue with agent, which likely limited the sensitivity of the study. Researchers studying capillary hemorrhage induced by contrast DUS with an older model DUS system resorted to a strategy of manually switching the scanner on and off each 10 s ten times, in order to crudely approximate intermittent scanning (Miller and Quddus, 2000). DUS-specific parameters can influence results in ways which might be unexpected or counter-intuitive. The time needed for a scanned beam to pass a point in tissue was shown to be important for GCH induced by contrast DUS: slower scan rates of Doppler imaging delivering a long sequence of pulses, which slowly ramped up in PRPA, produced a much lower effect than fast B mode scans (Miller et al. 2007b). Recently, we have developed a method to simulate DUS exposure of UCA *in vivo* by using a laboratory exposure system with amplitude modulation of a pulse train to mimic the image pulse sequences of intermittent DUS scanning (Miller et al. 2007c). This method employed damped focused transducers to create DUS-like fields in rat kidney, and exposure at several positions during contrast infusions to approximate the exposure of image scan planes in DUS.

The purpose of this study was to examine the frequency dependence of GCH by contrast aided diagnostic ultrasound in rats. Renal imaging is an important application of contrast aided diagnostic ultrasound (Wei et al. 2001; Robbin et al. 2003; Correas et al. 2006), and therefore the GCH bioeffect is directly relevant to the cavitation bioeffects problem in DUS safety assurance. Diagnostic ultrasound scanners were utilized to the extent possible, including the previously published work at 1.5 MHz (Miller et al. 2007a) and 2.5 MHz (Miller et al. 2007b). The laboratory exposure system was used to simulate diagnostic ultrasound exposure for higher PRPAs than those available with our diagnostic equipment. Exposures at frequencies of 1.0, 1.5, 2.25, 3.5, 5.0 and 7.5 MHz expanded the frequency range over which GCH induction could be observed. This research indicated a rapid increase of the magnitude of GCH above a threshold PRPA and an approximately linear frequency dependence of the GCH thresholds.

Materials and Methods

This study was designed to expose the right kidneys of rats with circulating UCA to different frequencies of pulsed ultrasound, under conditions which were intended to simulate reasonable worst-case clinical conditions in essential respects. The plan was developed as a model system for cavitation biology research, rather than as a replication of any specific contrast aided DUS examination. Both actual DUS scanners and laboratory transducers were used. The anesthetized rats were exposed to ultrasound in a water bath at normal focal distances. For each exposure source and frequency combination, groups of rats were exposed to a series of calibrated in situ values of the PRPA. The glomerular capillary hemorrhage (GCH) bioeffect was measured both by gross examination of the kidney surface, and by histological scoring in the center of the scan plane. The results were used to determine the occurrence of GCH as a function of PRPA including the apparent threshold for each source and frequency, and then to assess the frequency dependence of these thresholds and of the magnitude of the bioeffect above the thresholds.

This investigation was conducted with the approval of the University Committee on the Use and Care of Animals, University of Michigan. Hairless rats (CD hairless, Charles River Laboratories, Wilmington MA) were anesthetized by intramuscular injection of pentobarbital at a dose of 50 mg/kg. A 24 gauge cannula was inserted into a tail vein for UCA injections. The rats were mounted on their left side on a plastic holder, which was then mounted vertically in a bath of 37 °C degassed water with the rat's head above the water level. A total of 171 rats were used in this study with 163 yielding usable data (8 rats suffered anesthetic death or other problems, and were excluded from the study). In addition, the data from exposure-response tests using identical DUS exposure methods in three previous studies were incorporated into this study for comparison to the newer data. Data for 1.5 MHz DUS were included from 25 rats scanned with a tissue mimicking path (Miller et al. 2007a) and 6 rats scanned with a water-path (Miller et al. 2007c). Data for 2.5 MHz B mode flash echo imaging were included from 22 rats (Miller et al. 2007b).

Ultrasound exposure systems

Two exposure systems were used: a diagnostic ultrasound machine and a laboratory exposure system. The diagnostic machine was a GE Vingmed System V (General Electric Co., Cincinnati OH) with cardiac phased array probes. Some previously published results from the FPA 2.5 probe were included in this study for 1.5 MHz intermittent imaging (Miller et al. 2007a, c). In addition, previously published results obtained using a Powervision 8000 (model SSA-390A, Toshiba Corporation, Tochigi-Ken, JPN) with PVN-375AT probe were included in this study for data on 2.5 MHz intermittent imaging (B mode Flash Echo Imaging mode) (Miller et al. 2007b). Characteristics for each of the eleven exposure arrangements are listed in Table 1. As described previously, the probes were clamped in a water bath with the right kidney of a rat located at the focal zone (Miller et al. 2007a). The selected frequency in this study for the FPA 2.5 probe was 3.6 MHz (3.2 MHz actual frequency measured from the pulse waveform) with a 26 Hz frame rate. The selected frequencies for the FPA 10 probe were 5.0 MHz with a 68.1 frame rate and 10 MHz (7.4 MHz actual) with a 46.8 Hz frame rate. The scan rates were modified for exposure by the intermittent frame-trigger feature at a 1 s interval (e. g. a 26 Hz scan generated once per s). Even for intermittent imaging, the frame rate is important for determining the duration of the image pulse sequence (IPS) arriving at a point in the tissue as the scanning beam passes by, which is an important parameter for the GCH effect (Miller et al. 2007b). The IPSs were observed at the focal maximum and consisted of a sequence of pulses (of approximately equal pulse duration), which were separated by a fixed pulse repetition period and increased in amplitude to the peak (when the beam was aimed directly at the hydrophone) and then declined. The peak rarefactional pressure amplitude (PRPA) was

measured according to Miller et al. (2007c). This PRPA measurement was derated by an attenuation factor, which was measured by insertion of abdominal wall tissue samples from four rats between the probe and hydrophone, to provide the in situ value at the kidney. This derated value also was used for estimating the equivalent Mechanical Index (MI) of the exposures (which has relevance to the on-screen MI value in human clinical examinations). The thickness of the scan plane at the half PRPA (−6 dB) points were measured and are listed in Table I as the beam width (BW). To help characterize the IPS, the rarefactional pressure amplitudes were fitted with a 4 parameter Gaussian envelope (Sigmaplot 9.0, Systat Software Inc., Point Richmond CA USA), which was used to determine an IPS duration of each scan as the full width of the envelope at half the PRPA. The timing parameters needed to characterize the IPS were the pulse duration, pulse repetition period (PRP), IPS duration and image repetition period (set to 1 s), which are listed in Table 1.

The laboratory exposure system consisted of a transducer, power amplifier (A-500, Electronic Navigation Industries, Rochester NY), function generator (model 3314A function generator, Hewlett Packard Co., Palo Alto CA) and an arbitrary waveform generator (model 33220A, Agilent Technologies, Loveland CO). Six damped single element transducers (Panametrics, Olympus NDT Inc. Waltham, MA) with 1.9 cm diameter and 3.8 cm focus were used at their resonant ultrasonic frequencies of 1.0, 1.5, 2.25, 3.5, 5.0 and 7.5 MHz. The function generator was set using the n-cycle mode with n=3 to produce a simple pulse train with pulse durations and PRPs similar to those of DUS. The PRPAs were measured as described above, except that an additional adjustment was made for the reduction in apparent PRPA due to the finite size of the hydrophone, as described previously (Miller and Dou, 2004a). The beam widths listed in Table 1 were determined as the mean of the two perpendicular diameters at the half PRPA (−6 dB) points. The main purpose of the laboratory system was to allow exposure at higher PRPAs than were available with the DUS systems, and thereby extend the frequency range over which GCH could be detected (see Table 1). The arbitrary waveform generator was used to modulate the amplitudes of the pulse train from the function generator with a Gaussian function, in order to simulate the IPS of a DUS scan, as described previously (Miller et al. 2007c). The pulse durations, PRPs and IPS durations, which are given as the full width at half the peak PRPA of the Gaussian function, are listed in Table 1. The parameter values were chosen to give shorter pulses, PRPs and IPS durations for increasing ultrasound frequency, as expected for clinical DUS, but were not adjusted to duplicate any specific DUS system. The exposures with the laboratory system were aimed at the kidney pelvis with the aid of the DUS system with the FPA 10 probe operating at 8 MHz with default settings, as described previously (Miller et al. 2007c). Once the center of the right kidney was located, the DUS probe was shifted horizontally to position the laboratory transducer at the same place with its focal zone at the kidney cortex.

The single element damped transducers provided a simulation of the DUS pulse, PRP and IPS at a single focal line. Since the beam was fixed, exposure at only one position included a decreasing volume of kidney cortex as the transducer frequency increased and beam width decreased (see Table 1). In order to compensate for this volume effect to some extent, only the 1.0 MHz transducer was used in one position. The other laboratory transducers were used to expose the kidney at multiple positions, which were spaced horizontally at approximately the −3 dB diameter (i. e. the half power beam width) of the beams, as listed in Table 1. For example, the 5.0 MHz transducer was used to expose the kidney at six positions, for a total of 6 min. The evaluation of the resulting bioeffects examined the effects within a cross section passing through all the exposed positions (as for a scan plane). The multi-position method served to treat an approximately constant horizontal segment of the cortex cross section on the proximal side of the kidney for the six laboratory transducers. For example, kidneys exposed by this scheme at 1 MHz with one position and 5.0 MHz at six positions are shown in Fig. 1a and Fig. 1b, respectively. The regions impacted by exposure with GCH and with blood filled tubules

visible on the surface are somewhat broadened due to a vertical breathing motion imposed on the kidney; however, the horizontal extent of the effected areas are approximately the same. Of course, this exposure scheme did not generate a band of blood-filled tubules extending completely around the kidney, as was seen for DUS scans (Miller et al. 2007a,b).

Ultrasound Contrast Agent Infusion

A clinical diagnostic UCA (Definity®, Bristol-Myers Squibb Medical Imaging, Inc., N. Billerica, MA USA) was purchased from the manufacturer and a fresh vial was prepared each day according to the manufacturer's instructions. For infusion, 60 µl of the agent was diluted in a syringe containing 3 ml of sterile saline and used to fill a 30 cm extension tube with the diluted agent mounted in a syringe pump. With the rat mounted in a water bath, the syringe was mounted on a syringe pump and the extension tube was connected to the tail vein cannula. The diluted agent was then infused at 0.5 ml/kg/min, which equals an infusion rate of 10 µl/kg/min of the undiluted agent. Exposure was begun 15 s after starting the infusion (to allow agent to begin circulating) and continued for the duration of the exposure (listed in Table 2).

Evaluation of Glomerular Capillary Hemorrhage

The rats were removed from the water bath and mounting board after contrast ultrasound exposure and the kidney was removed after approximately 5 min. The kidneys were trimmed to a transverse section about 5 mm thick, which contained the exposed central portion of the kidney, and placed in buffered 10% formalin fixative. After 5–7 days, the samples were trimmed again to fit into the histological processing cassettes with guidance from any surface petechiae of blood filled tubules (e. g. see Fig. 1) and then processed for histology. The percentage of glomeruli with red blood cells in the Bowman's space was counted in histological sections, as described previously (Miller et al. 2007a). Briefly, histological slides from the center of the scan plane were scored blind using a 20x objective on a light microscope (model DMRB, Leica Inc., Deerfield IL USA). The percentage of glomeruli with GCH was determined for the entire section for DUS exposure and for the beam entrance area within the renal cortex for the laboratory system. The later method ignored any GCH on the beam exit side of the kidney, because the position of this region varied from cortex to the renal pelvis (containing no glomeruli). In addition, the kidney surface was observed grossly (e. g. Fig. 1) and any petechiae formed by blood-filled tubules, which was indicative of GCH, were noted and counted for low numbers of petechiae. Quantitative histological scoring was performed for all of the DUS-exposed samples. For the samples exposed with the laboratory system, only samples from exposure conditions yielding evidence of GCH on the surface (except for 5 sham exposed samples, for a total of 102 samples examined histologically), because previous experience showed that there was no possibility of finding hidden GCH when no blood-filled tubules were evident. The gross observation was not quantitative with respect to the percentage of GCH, but provided valuable qualitative information as to whether or not any GCH had occurred.

Experimental Plan and Statistics

For each source and frequency condition, a series of PRPA levels were chosen approximately 3 dB (a factor of two in acoustical power) apart, which included the maximum available peak PRPA. Five rats were exposed at each level with replacements for the few excluded rats (noted above), except for one condition limited to 3 rats, because the next higher level had no effect. The lowest level tested was selected on the basis of the previous work, and included at least one level with all five samples showing no GCH. A total of 5 groups were tested for the DUS system (plus the previous data noted above), and 27 groups for the laboratory system. Numerical results are presented as the mean plus/minus one standard deviation, or plotted as the mean with standard error bars. For statistical analysis, Student's t-tests or Mann-Whitney

rank sum tests were used as appropriate to compare means of the measured parameters, with statistical significance assumed at P=0.05. The apparent threshold for each source and frequency condition was taken either to be midway between the lowest level with a significant percentage of GCH, and the next lower level, or to be at the lowest level with a significant number of visible petechiae from blood filled tubules on the surface. This method was followed to establish thresholds which did not have any significant effect at levels below the threshold (which may occur for force fitting of simple threshold functions such as a hockey-stick function). Trends in the data were assessed by linear regression.

Results

GCH was evaluated as the percentage of glomeruli with evidence of blood in Bowman's (urinary) space in a histological section from the center of the exposure plane. The percentages of GCH versus PRPA are plotted for the DUS systems in Fig. 2 (top). The three lowest frequencies gave typical exposure response curves with a sharp rise above apparent thresholds. The thresholds and other parameters are listed in Table 2. For the two highest frequencies, even the highest available PRPA did not yield any significant GCH by either histology or visual inspection. It should be noted that the highest available PRPAs at 5 MHz and 7.4 MHz with the GE Vingmed system were 2.6 MPa and 2.9 MPa, respectively, which are well below the upper limit for DUS (4.2 MPa and 5.2 MPa, respectively at MI=1.9).

The percentages of GCH versus PRPA are plotted for the six frequencies of the laboratory system in Fig. 2 (bottom). Again, each frequency gave a typical exposure-response trend similar to the DUS results (at the lower frequencies), and the apparent thresholds are listed in Table 2. Near the apparent threshold for GCH, the effect was also measured by counting the number of surface petechiae of blood filled tubules, which were often present for the highest PRPA with no significant percentage of GCH in histology. This reflects the sensitivity of the simple visual inspection of the kidney surface for low incidence of GCH. For the 7.5 MHz transducer, the GCH seen in histology was not statistically significant for the highest available PRPA, but the surface petechiae were significant at this PRPA.

The apparent thresholds increased steadily with increasing frequency. These are listed in Table 2 and plotted for the DUS conditions in Figure 3. The thresholds are substantially below the upper limit of MI=1.9 for the lower frequencies. In this plot with logarithmic scales, the linear dependence of the threshold p_t on frequency f is evident. The solid line is a linear regression on the three data for frequencies with bioeffects of the form

$$p_t=bf^a \qquad (1)$$

in which b=0.49 MPa/MHz, and a=1.05 with r^2=0.99. This excellent correlation coefficient lends confidence in the linear relationship over this narrow frequency range; however, the 95% confidence limits, which are plotted as the two dotted curves, indicate substantial uncertainty in the linear relationship (e. g. a=0.5 or a=2 might lie within the confidence limits). The apparent thresholds for the different laboratory system frequencies are plotted in Fig. 4. Again a linear regression (Eq. 1) yielded a good fit to the data for b=0.62 and a=1.04 with r^2=0.98. The thresholds were slightly higher than those for the DUS system, which probably reflects the smaller region of tissue exposed to the peak PRPA for the fixed transducer system (i. e., a series of beam lines, rather than a plane for the DUS scans). The 95% confidence limits are much tighter in this case, owing to the broader frequency range covered by the laboratory system (e. g., these confidence limits rule out a=0.5). The uncertainty in the data points may be taken to be about ±1.5 dB on the logarithmic scale, because the steps in the exposure levels were increments of 3 dB. This uncertainty is illustrated by error bars on the 1.5 MHz data point, and is commensurate with the 95% confidence limits of the linear regression.

The statistical evaluation of the increasing thresholds for GCH with increasing ultrasonic frequency indicated that the relationship was approximately linear. Assuming that the exponent a was exactly 1, then the ratio p_t/f was approximately equal to the constant b. This suggests that the PRPA divided by the ultrasonic frequency (p_r/f) may be a useful exposure parameter for characterizing this bioeffect. The utility of this parameter is illustrated in Fig. 5, which is a re-plotting of the GCH data from Fig. 2 against p_r/f (rather than simply p_r). In Fig. 5 the great spread of the data for different frequencies in Fig. 2, collapses to a much narrower range, with many of the error bars overlapping for data at different frequencies. A small departure from this general trend occurred for the 1.0 MHz laboratory system data, which fell below the other data (i. e. less effective). This departure may reflect the rather low frequency relative to diagnostic ultrasound and the availability of optimum gas bodies. The optimal size is expected to increase for decreasing ultrasonic frequency. For 1 MHz, optimum nuclei may not exist in large numbers for Definity® infusion, particularly after passage through the lung circulation.

Discussion and Summary

The ultrasonic frequency dependence of glomerular capillary hemorrhage (GCH) induced by diagnostic ultrasound with contrast agent was investigated. Both diagnostic ultrasound (DUS) machines and a laboratory exposure system, which simulated DUS exposure with extended ranges of exposure PRPA, were used for exposure of rat kidneys. The exposure-response trend was a rapid rise in percentage of GCH with PRPA above an apparent threshold p_t, see Fig. 2. The thresholds were defined at each frequency with detectable GCH as the lowest PRPA for significant indications of the effect (see Methods). Results for the DUS frequencies indicated a linear dependence of PRPA threshold on frequency, which was approximately $p_t = 0.5 f$ (Fig. 3). To avoid the GCH bioeffect, DUS modes for use with contrast agents could be limited to $p_r/f < 0.5$. However, the limited frequency range of 1.5–3.2 MHz, for which the bioeffect could be observed with DUS exposure, limited the confidence in this functional dependence. The laboratory system was used to simulate intermittent DUS image pulse sequences for six frequencies. The results again indicated a linear dependence of PRPA thresholds on frequency with $p_t = 0.6 f$ (Fig. 4), which provided confirmation of the linear dependence over the range 1.0–7.5 MHz. This functional dependence of apparent thresholds has also been noted for several *in vitro* bioeffects (Miller and Dou, 2004a;Miller et al. in press), which implies that this parameter may have a broader significance in ultrasonic cavitation biology. Plotting the percentage of GCH against the parameter p_r/f collapsed the disparate exposure-response curves into a tight grouping (Fig. 5), which indicates that this parameter carries predictive value even for the frequency dependence of the magnitude of GCH above the threshold. This magnitude increases rapidly with increasing p_r/f. The percentage GCH data (omitting the 1 MHz data set, and data means equal to zero) versus p_r/f in a logarithmic plot had a linear regression slope of 4.2 (r^2=0.89), which indicates a dependence approximately of the form $(p_r/f)^4$ above the threshold.

The Mechanical Index (MI) parameter, which has the form $p_r/f^{1/2}$, has an incorrect frequency dependence for describing GCH, see Fig. 3 and Fig. 4. In addition, the upper limit of 1.9 on the MI does not provide assurance that GCH would not occur in DUS examinations. At 1.5 MHz, the DUS threshold was found to be 0.95 MPa, which corresponds to MI=0.78, a factor of 2.4 (7.8 dB) lower than the upper limit. The MI was derived from theory for optimal nucleation of cavitation; however, the theoretical prediction of the inertial cavitation threshold in blood (Apfel and Holland, 1991) (Fig. 3 and Fig. 4) falls well below the GCH thresholds at the higher frequencies. The bioeffects thresholds apparently depend on other processes in addition to the threshold for inertial collapse cavitation. The MI has also been found to be of little value for forecasting gas body destruction and the loss of image contrast (Forsberg et al. 2006), which may be related to cavitation nucleation.

As discussed in a previous report (Williams et al. 2007), the characteristics of rat and human glomerular capillaries are about the same and, therefore, GCH would be expected to occur in human clinical examinations if the same agent dose and ultrasound exposure reached the human kidney as reached the rat kidney in this study. Estimates of the equivalent threshold MI values, relevant to the on-screen MI, have been listed in Table 2. However, it should be noted that the on-screen MI may not accurately specify the exposure in a kidney during a clinical examination. For example, obese patients may have significantly greater attenuation than assumed in the MI calculation. In addition, the laboratory system exposures used here exceeded the upper limits of DUS for the higher PRPA values. The increasing thresholds with increasing frequency limited the GCH effect for contrast aided DUS, and no GCH was seen for DUS at 5.0 or 7.4 MHz for the highest available PRPAs. Since the threshold at 7.5 MHz was greater than the USFDA upper limit guideline of MI=1.9, the GCH effect would not be expected to occur for a clinical examination, with other parameters similar to those used in this study, at frequencies of 7.5 MHz or above.

The results of this study accentuate the need for continual revaluation of the safety assurance framework for diagnostic ultrasound. The need appears to be particularly acute with respect to the cavitation mechanism for bioeffects studied herein, because bioeffects likely could occur in the clinical setting for existing ultrasound machines and contrast agents. The upper limit for the MI exposure parameter fails in its safety assurance role because bioeffects occur at lower levels. The need for reconsideration of the safety assurance framework for DUS arises from other bioeffects findings as well. Lung hemorrhage is also possible with present diagnostic ultrasound machines (AIUM, 2000). The MI does not apply to this bioeffect, because it does not depend on the inertial cavitation mechanism (Raeman et al. 1997; O'Brien et al. 2000). Data on lung hemorrhage has been used to propose a complex new index for this bioeffect, which includes timing parameters (Church and O'Brien, 2007). Furthermore, the establishment of rigid upper limits for diagnostic ultrasound machines has become a matter of debate (O'Brien and Miller, 2001; O'Brien et al. 2002), because the unscientific limits were based on the state-of-the-art for pre-1976 DUS. As medical ultrasound evolves and research related to safety accumulates, safety assurance parameters should be developed and adjusted on a scientific basis. Different exposure indices and limits might be appropriate for qualitatively different types of examinations, such as for contrast enhanced DUS.

Acknowledgment

References

AIUM/NEMA. Standard for Real-Time Display of Thermal and Mechanical Acoustic Output Indices on Diagnostic Ultrasound Equipment. Rockville MD: American Institute of Ultrasound in Medicine; 1992. p. 1-58.

AIUM. Mechanical Bioeffects from Diagnostic Ultrasound: AIUM Consensus Statements. J. Ultrasound Med 2000;19:67–168.

Albrecht T, Blomley M, Bolondi L, Claudon M, Correas JM, Cosgrove D, Greiner L, Jäger K, Jong ND, Leen E, Lencioni R, Lindsell D, Martegani A, Solbiati L, Thorelius L, Tranquart F, Weskott HP, Whittingham T. EFSUMB Study Group. Guidelines for the use of contrast agents in ultrasound. January 2004. Ultraschall Med 2004;25:249–256. [PubMed: 15300497]

Apfel RE, Holland CK. Gauging the likelihood of cavitation from short-pulse, low-duty cycle diagnostic ultrasound. Ultrasound Med. & Biol 1991;17:179–185. [PubMed: 2053214]

Averkiou M, Powers J, Skyba D, Bruce M, Jensen S. Ultrasound contrast imaging research. Ultrasound Q 2003;19:27–37. [PubMed: 12970614]

Blomley M, Claudon M, Cosgrove D. WFUMB Safety Symposium on Ultrasound Contrast Agents: clinical applications and safety concerns. Ultrasound Med Biol 2007;33:180–186. [PubMed: 17254696]

Church CC, O'Brien WD Jr. Evaluation of the threshold for lung hemorrhage by diagnostic ultrasound and a proposed new safety index. Ultrasound Med Biol 2007;33:810–818. [PubMed: 17383801]

Correas J-M, Claudon M, Tranquart F, Helenon O. Ultrasound contrast agents: properties, principles of action, tolerance, and artifacts. Eur Radiol 2001;11:1316–1328. [PubMed: 11519538]

Dalecki D. WFUMB safety symposium on echo-contrast agents: Bioeffects of ultrasound contrast agents *in vivo*. Ultrasound Med Biol 2007;33:205–213. [PubMed: 17239521]

Dalecki D, Raeman CH, Child SZ, Cox C, Francis CW, Meltzer RS, Carstensen EL. Hemolysis *in vivo* from exposure to pulsed ultrasound. Ultrasound Med Biol 1997;23:307–313. [PubMed: 9140187]

FDA. Information for Manufacturers Seeking Marketing Clearance of Diagnostic Ultrasound Systems and Transducers. Rockville MD: Food and Drug Administration; 1997. p. 1-1-G-4

Forsberg F, Merton DA, Goldberg BB. *In vivo* destruction of ultrasound contrast microbubbles is independent of the mechanical index. J Ultrasound Med 2006;25:143–144. [PubMed: 16371568]

Greenbaum L, Burns P, Copel J, Cosgrove D, Fowlkes JB, Goldberg B, Mattrey R, Merton D, Robbin M, Wilson S. American Institute of ultrasound in Medicine recommendations for contrast-enhanced liver ultrasound imaging clinical trials. J Ultrasound Med 2007;26:705–716. [PubMed: 17526602]

Miller DL, Dou C. Membrane damage thresholds for 1- to 10-MHz pulsed ultrasound exposure of phagocytic cells loaded with contrast agent gas bodies *in vitro*. Ultrasound Med. Biol 2004a;30:973–977. [PubMed: 15313329]

Miller DL, Dou C. Theoretical gas body pulsation in relation to empirical gas-body destabilization and to cell membrane damage thresholds. J. Acoust. Soc. Am 2004b;116:3742–3749. [PubMed: 15658724]

Miller DL, Gies RA. The influence of ultrasound frequency and gas-body composition on the contrast agent-mediated enhancement of vascular bioeffects in mouse intestine. Ultrasound Med. Biol 2000;26:307–313. [PubMed: 10722920]

Miller DL, Quddus J. Diagnostic ultrasound activation of contrast agent gas bodies induces capillary rupture in mice. Proc. Nat. Acad. Sci 2000;97:10179–10184. [PubMed: 10954753]

Miller D, Thomas R. Ultrasound contrast agents nucleate inertial cavitation *in vitro*. Ultrasound Med. & Biol 1995;21:1059–1065. [PubMed: 8553500]

Miller DL, Gies RA, Chrisler W. Ultrasonically induced hemolysis at high cell and gas body concentrations in a thin-disc exposure chamber. Ultrasound Med. & Biol 1997;23:625–633. [PubMed: 9232772]

Miller DL, Dou C, Wiggins RC, Wharram B, Goyal M, Williams AR. An *in vivo* rat model simulating imaging of human kidney by diagnostic ultrasound with gas-body contrast agent. Ultrasound Med Biol 2007a;33:129–135. [PubMed: 17189055]

Miller DL, Dou C, Wiggins RC. Doppler mode pulse sequences mitigate glomerular capillary hemorrhage in contrast-aided diagnostic ultrasound of rat kidney. IEEE Trans. UFFC 2007b;54:1802–1810.

Miller DL, Dou C, Wiggins RC. Simulation of diagnostic ultrasound image pulse sequences in cavitation bioeffects research. J Acoust Soc Am 2007c;122:2002–2008. [PubMed: 17902837]

Miller DL, Averkiou M, Brayman A, Everbach E, Holland C, Wible J, Wu J. Bioeffects considerations for diagnostic ultrasound contrast agents. J Ultrasound Med. (in press)

NCRP Exposure Criteria for Medical Diagnostic Ultrasound: II. Criteria Based on All Known Mechanisms Report No. 140. Bethesda Md.: National Council on Radiation Protection and Measurements; 2002. p. 1-574.

O'Brien WD Jr, Miller D. Diagnostic ultrasound should be performed without upper intensity limits. Med Phys 2001;28:1–3. [PubMed: 11213914]

O'Brien WD Jr, Frizzell LA, Weigel RM, Zachary JF. Ultrasound-induced lung hemorrhage is not caused by inertial cavitation. J Acoust Soc Am 2000;108:1290–1297. [PubMed: 11008829]

O'Brien WD Jr, Abbott JG, Stratmeyer ME, Harris GR, Schafer ME, Siddiqi TA, Merritt CR, Duck FA, Bendick PJ. Acoustic output upper limits proposition: should upper limits be retained? J Ultrasound Med 2002;21:1335–1341. [PubMed: 12494975]

Porter TR, Everbach C, Kricsfeld D, Xie F. Myocardial cavitational activity during continuous infusion and bolus intravenous injections of perfluorocarbon-containing microbubbles. J Am Soc Echocardiogr 2001;14:618–625. [PubMed: 11391291]

Raeman CH, Dalecki D, Child SZ, Meltzer RS, Carstensen EL. Albunex does not increase the sensitivity of the lung to pulsed ultrasound. Echocardiography 1997;14:553–558. [PubMed: 11174994]

Raisinghani A, Rafter P, Phillips P, Vannan MA, DeMaria AN. Microbubble contrast agents for echocardiography: rationale, composition, ultrasound interactions, and safety. Cardiol Clin 2004;22:171–180. [PubMed: 15158932]

Robbin ML, Lockhart ME, Barr RG. Renal imaging with ultrasound contrast: current status. Radiol Clin North Am 2003;41:963–978. [PubMed: 14521204]

Wei K, Le E, Bin JP, Coggins M, Thorpe J, Kaul S. Quantification of renal blood flow with contrast-enhanced ultrasound. J Am Coll Cardiol 2001;37:1135–1140. [PubMed: 11263620]

Wible J Jr, Galen K, Wojdyla J, Hughes M, Klibanov A, Brandenburger G. Microbubbles induce renal hemorrhage when exposed to diagnostic ultrasound in anesthetized rats. Ultrasound Med Biol 2002;28:1535–1546. [PubMed: 12498949]

Williams AR, Wiggins RC, Wharram BL, Goyal M, Dou C, Johnson KJ, Miller DL. Nephron injury induced by diagnostic ultrasound imaging at high mechanical index with gas body contrast agent. Ultrasound Med Biol 2007;33:1336–1344. [PubMed: 17507144]
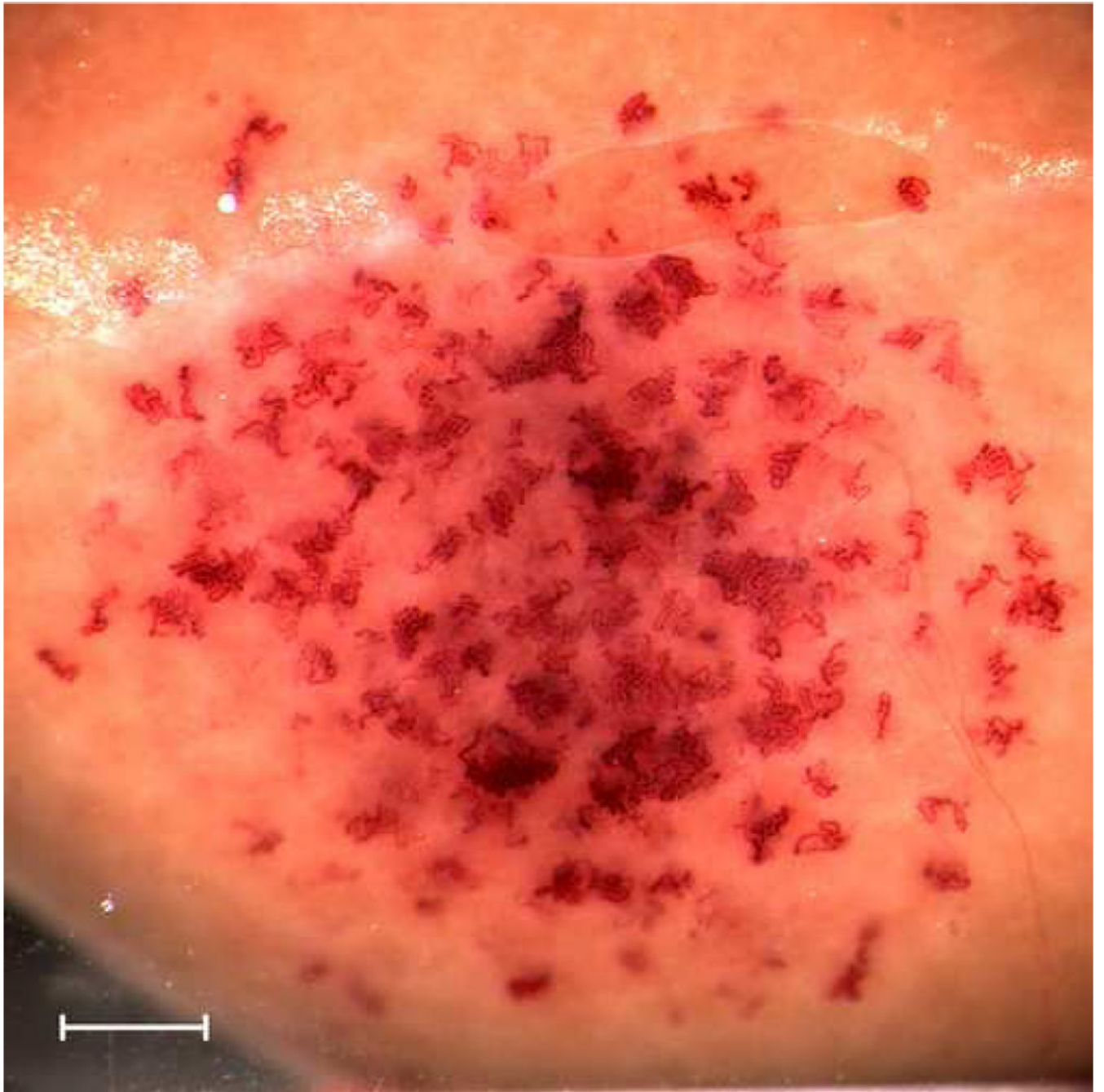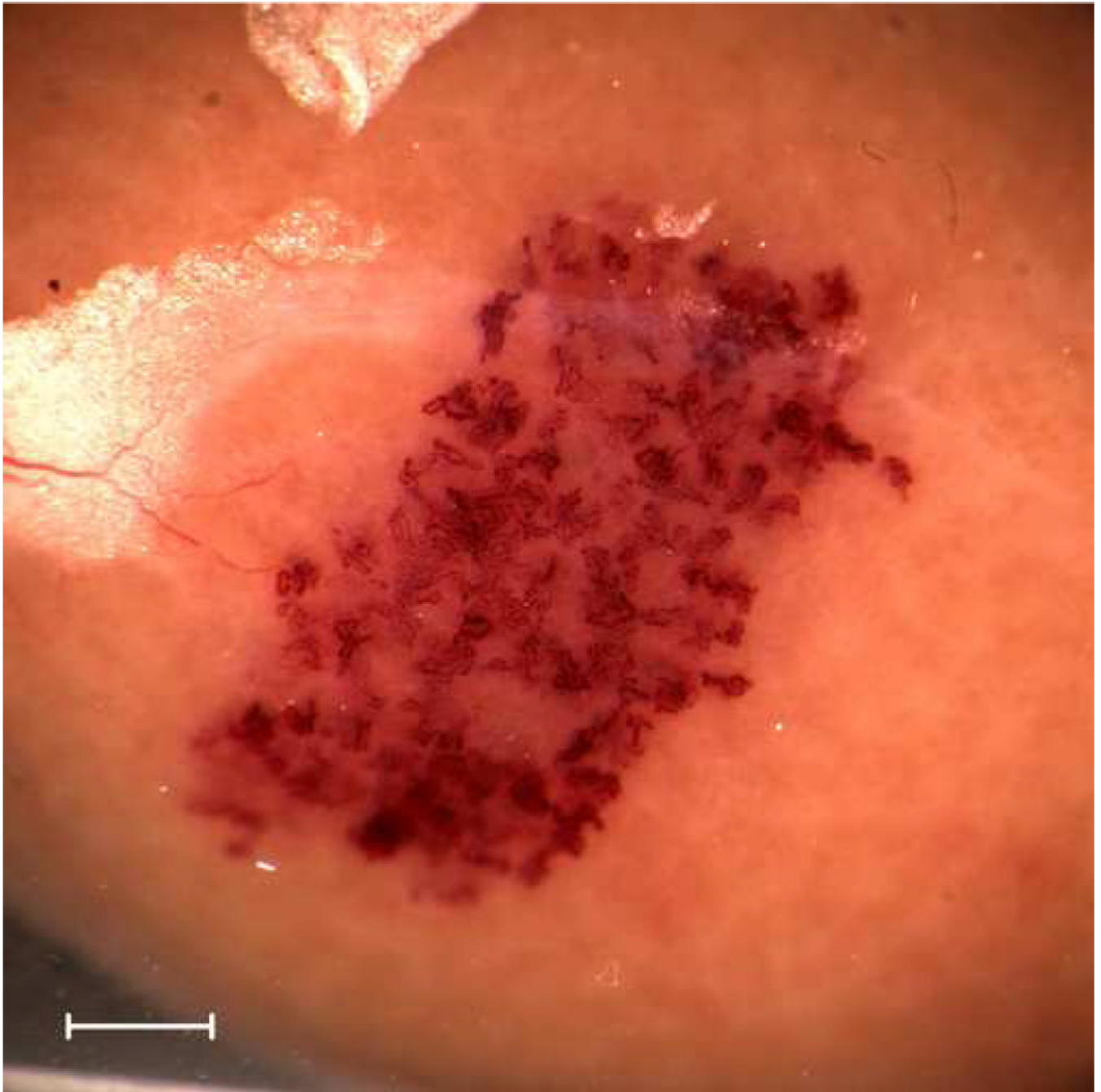
1.
Gross photographs of kidneys exposed with the laboratory system at the highest available rarefactional pressure amplitudes showing the extent of the effected regions on the surface. For 1 MHz (top), the exposure was at one position of the fixed beam. For 5 MHz (bottom), exposures were made at six adjacent positions along a scan line in order to cover a distance along the line similar to that covered by the single 1 MHz exposure. Scale bars: 1 mm.
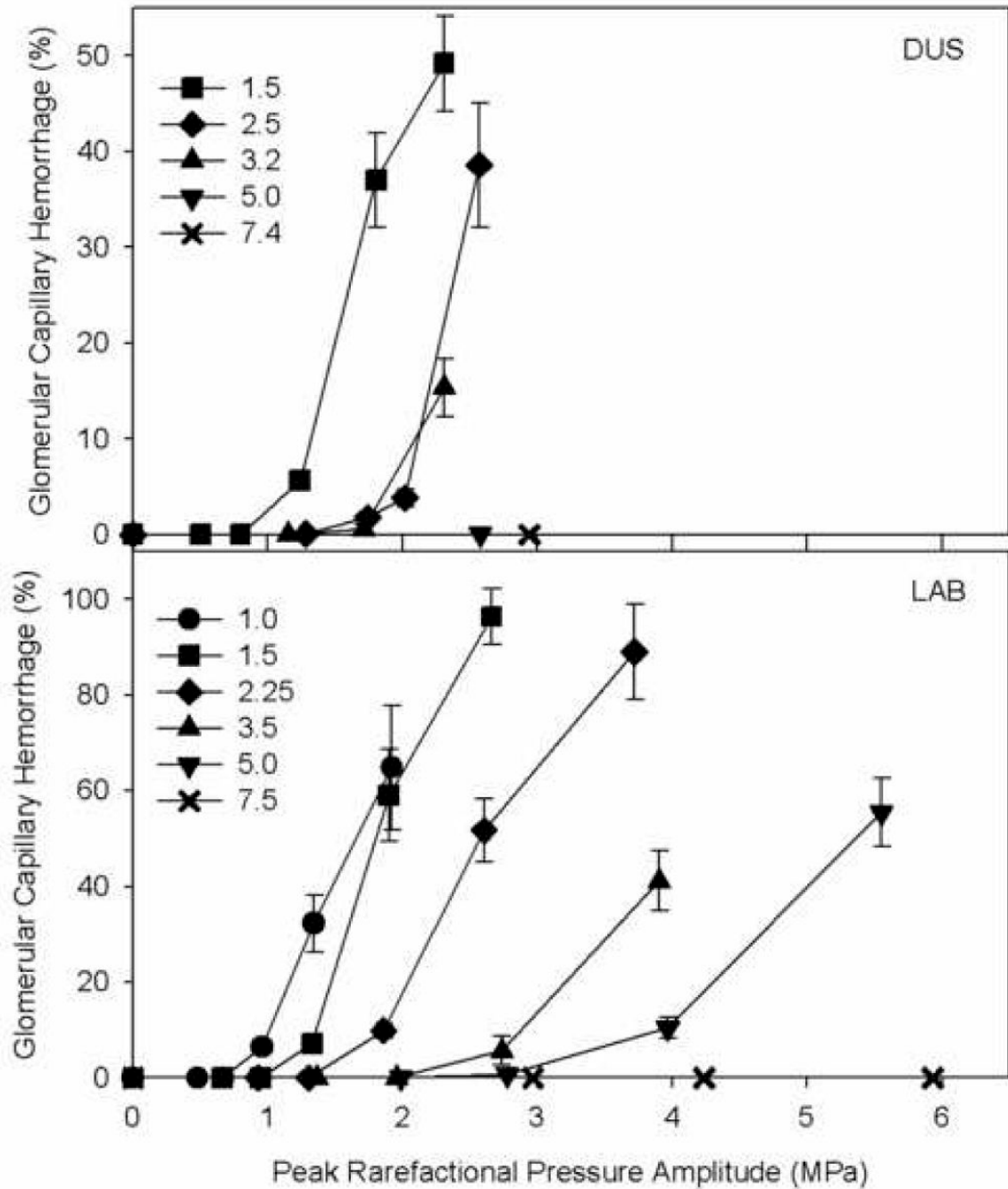
2.
The percentage of glomerular capillary hemorrhage (GCH) from histology for the different ultrasound frequency sources, each plotted as a function of the peak rarefactional pressure amplitude (PRPA). Typically, the bioeffect increased rapidly above an apparent threshold both for diagnostic ultrasound (DUS) exposure and for laboratory system (LAB) exposure. For the DUS at 5.0 MHz and 7.4 MHz, no GCH was induced even for the highest available PRPA. For the LAB at 7.5 MHz, the GCH was not significant for the histological evaluation (although GCH was evidenced by blood filled tubules grossly visible on the surface of the kidneys).
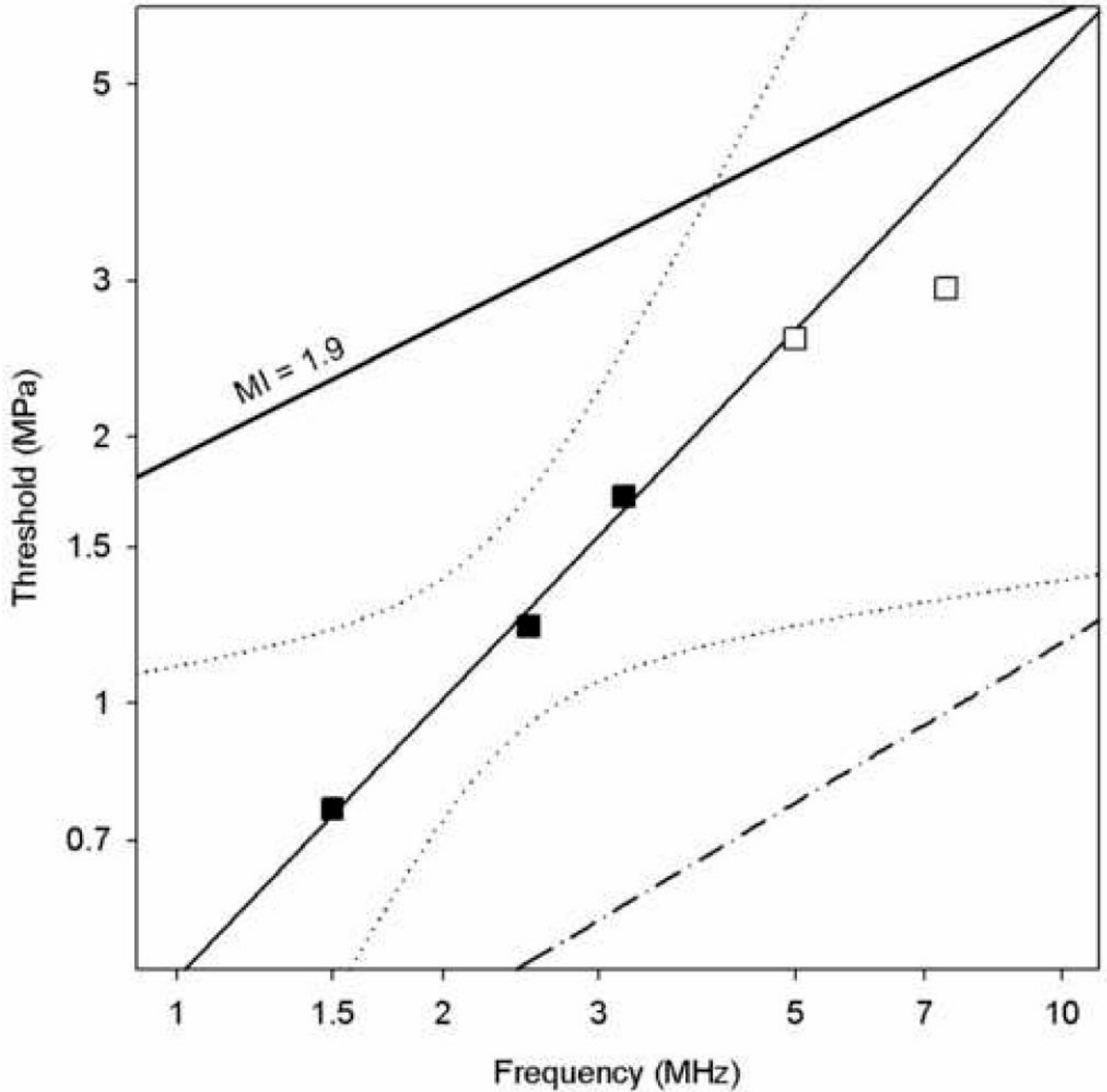
3.

Apparent thresholds for the diagnostic ultrasound exposures in terms of the peak rarefactional pressure amplitude (PRPA) plotted against the ultrasonic frequency of the source. The filled squares show the result for the frequencies with significant glomerular capillary hemorrhage (GCH), while the empty squares show the highest PRPAs available at the frequencies for which no significant GCH was seen. The solid line fitted to the data by linear regression has with 95% confidence limits shown as dotted curves. The line labeled MI=1.9 represents the upper limit for the Mechanical Index in diagnostic ultrasound, and the dash-dot line represent the theoretical prediction of cavitation thresholds in blood (Apfel and Holland, 1991).
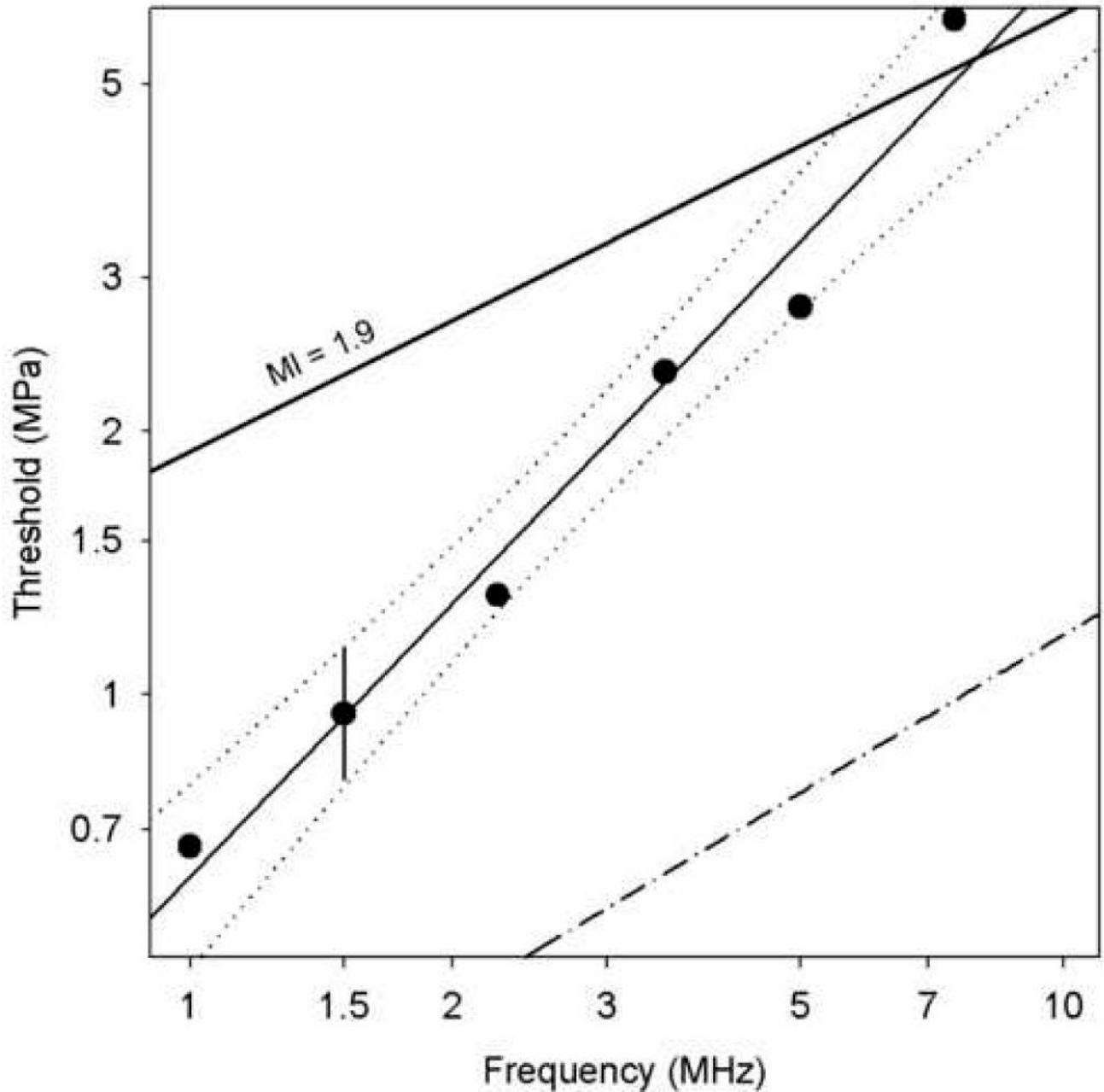
4.
Apparent thresholds of glomerular capillary hemorrhage for the laboratory-system exposures
in terms of the peak rarefactional pressure amplitude (PRPA) plotted against the ultrasonic
frequency of the transducers. The error bars on the 1.5 MHz data point illustrated the
uncertainty due to the step size between exposure levels. The solid line fitted to the data by
linear regression has 95% confidence limits shown as dotted curves, which lends support for
the approximate proportionality of the PRPA thresholds to the ultrasonic frequency. The line
labeled MI=1.9 represents the upper limit for the Mechanical Index in diagnostic ultrasound,
and the dash-dot line represent the theoretical prediction of cavitation thresholds in blood
(Apfel and Holland, 1991).
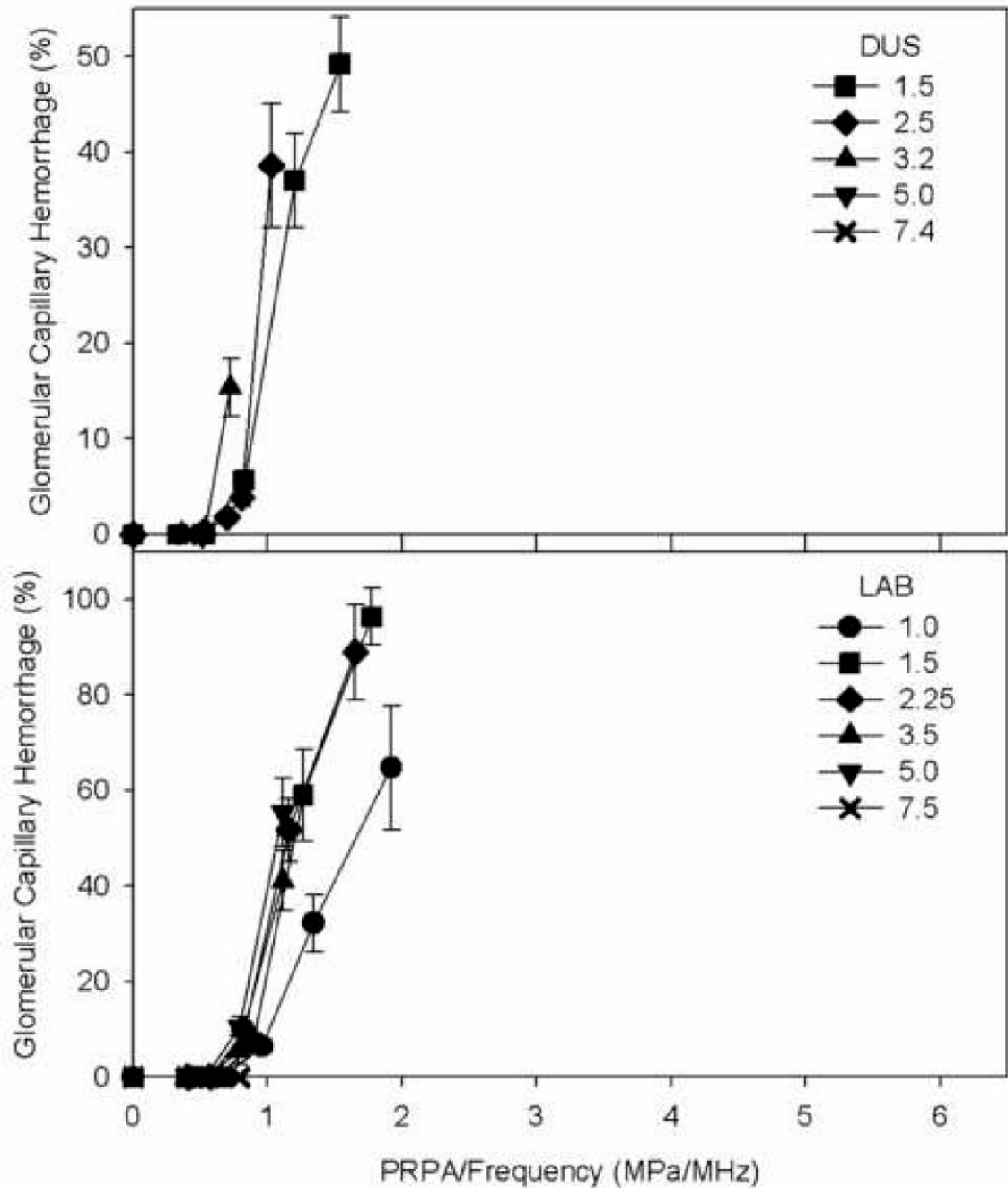
5.
The percentage of glomerular capillary hemorrhage (GCH) from histology as shown in Fig. 2, but replotted as a function of the peak rarefactional pressure amplitude (PRPA) divided by the ultrasonic frequency. The disparate curves in Fig. 2 collapse into a more consistent exposure-response when plotted against this PRPA/frequency exposure parameter.

Table 1

Ultrasonic sources and exposure parameters. The abbreviations are for frequency (Freq), duration (Dur.), pulse repetition period (PRP), beam width (B. W.), image pulse sequence (IPS), attenuation (Attn.), hydrophone corrections (Hydro. Corr.), and rarefactional pressure amplitude (RPA). The sources include laboratory transducers (LAB), and diagnostic ultrasound probes from the GE Vingmed system (FPA) and from the Toshiba system (PVN) (see text).

Source	Freq	Focus	Pulse Dur.	PRP	−6 dB B. W.	IPS Dur.	Atten.	Hydro. Corr.	Peak RPA
	MHz	cm	µs	µs	mm	ms	%	%	MPa
LAB 1.0	1.0	3.8	2.7	540	5.6	5.4	96 ± 1	100	1.9
LAB 1.5	1.5	3.8	1.8	360	3.5	3.6	95 ± 2	100	2.7
FPA 2.5	1.5	5.0	1.5	430	4.3	4.6	95 ± 2	100	2.3
LAB 2.25	2.3	3.8	1.18	240	2.35	2.4	93 ± 2	100	3.7
PVN-375AT	2.5	5.0	0.66	106	3.0	0.53	94 ± 3	100	2.6
FPA 2.5	3.2	3.0	1.07	364	5.0	1.4	93 ± 2	100	2.3
LAB 3.5	3.5	3.8	0.87	170	1.45	1.7	93 ± 2	105	3.9
FPA 10	5.0	3.0	0.5	166	1.9	1.48	89 ± 2	100	2.6
LAB 5.0	5.0	3.8	0.54	100	1.1	1.0	91 ± 3	109	5.6
FPA 10	7.4	3.0	0.34	166	1.0	1.1	89 ± 2	100	2.9
LAB 7.5	7.5	3.8	0.4	80	0.77	0.8	88 ± 2	119	5.9

Table 2

Ultrasonic exposure parameters and threshold results. MI is the estimated equivalent on-screen Mechanical Index. The sources include laboratory transducers (LAB), and diagnostic ultrasound probes from the GE Vingmed system (FPA) and from the Toshiba system (PVN) (see text).

Source	Frequency MHz	Exposure Duration min	Position Spacing mm	Threshold MPa	Threshold MI	Threshold MPa/MHz
LAB 1.0	1.0	1	-	0.67	0.67	0.67
LAB 1.5	1.5	2	2.6	0.95	0.78	0.63
FPA 2.5	1.5	1	-	0.76	0.62	0.51
LAB 2.25	2.3	3	1.8	1.3	0.87	0.58
PVN-375AT	2.5	1	-	1.22	0.76	0.48
FPA 2.5	3.2	1	-	1.71	0.96	0.53
LAB 3.5	3.5	4	1.1	2.34	1.25	0.67
FPA 10	5.0	1	-	-	-	-
LAB 5.0	5.0	6	0.8	2.78	1.24	0.56
FPA 10	7.4	1	-	-	-	-
LAB 7.5	7.5	9	0.5	5.93	2.16	0.79